

Probabilistic methods for approximate archetypal analysis

Ruijian Han^{*1}, Braxton Osting², Dong Wang³, and Yiming Xu^{*2,4}

¹Department of Statistics, The Chinese University of Hong Kong, Hong Kong

²Department of Mathematics, University of Utah, Salt Lake City

³School of Science and Engineering, The Chinese University of Hong Kong, Shenzhen

⁴Scientific Computing and Imaging Institute, University of Utah, Salt Lake City

Abstract

Archetypal analysis is an unsupervised learning method for exploratory data analysis. One major challenge that limits the applicability of archetypal analysis in practice is the inherent computational complexity of the existing algorithms. In this paper, we provide a novel approximation approach to partially address this issue. Utilizing probabilistic ideas from high-dimensional geometry, we introduce two preprocessing techniques to reduce the dimension and representation cardinality of the data, respectively. We prove that, provided the data is approximately embedded in a low-dimensional linear subspace and the convex hull of the corresponding representations is well approximated by a polytope with a few vertices, our method can effectively reduce the scaling of archetypal analysis. Moreover, the solution of the reduced problem is near-optimal in terms of prediction errors. Our approach can be combined with other acceleration techniques to further mitigate the intrinsic complexity of archetypal analysis. We demonstrate the usefulness of our results by applying our method to summarize several moderately large-scale datasets.

Keywords: Alternating minimization, Approximate convex hulls, Archetypal analysis, Dimensionality reduction, Random projections, Randomized SVD

1 Introduction

Archetypal analysis (AA) is an unsupervised learning method introduced by Cutler and Breiman in 1994 [9]. For fixed $k \in \mathbb{N}$, the method finds a convex polytope with k vertices, referred to as *archetypes*, in

^{*}Equal contribution.

the convex hull of the data that explains the most variation of the data. Equivalently, given $\{x_i\}_{i \in [N]} \subset \mathbb{R}^d$, AA can be formulated as the following optimization problem:

$$\min_{\mathbf{A} \in \mathbb{R}_{\text{cs}}^{N \times k}, \mathbf{B} \in \mathbb{R}_{\text{cs}}^{k \times N}} \frac{1}{\sqrt{N}} \|\mathbf{X} - \mathbf{XAB}\|_F \quad \mathbf{X} = [x_1, \dots, x_N] \in \mathbb{R}^{d \times N}, \quad (1.1)$$

where F denotes the Frobenius norm, and ‘cs’ stands for column stochastic matrices. The normalizing factor $\frac{1}{\sqrt{N}}$ is introduced for convenience later. To understand this formulation, note that the columns of \mathbf{XA} are the expected archetypes, and the columns of \mathbf{B} correspond to the projection coefficients of the columns of \mathbf{X} to the convex hull of the archetypes. Consequently, the objective defined in (1.1) represents the (average) variation of the data that cannot be explained by the convex combinations of the archetypes.

AA is closely related to other unsupervised learning methods such as the k -means, principal component analysis (PCA) and nonnegative matrix factorization (NMF) [18, 22]. In fact, AA can be seen as an interpolation between the k -means and PCA; it has more geometry than the former while includes convexity constraints when compared to the latter. This allows AA to produce more interpretable results in many applications, e.g., in evolutionary biology [38], meanwhile raising additional questions of increased computational complexity. Under suitable assumptions, the consistency and convergence of AA have recently been established in [31], laying the foundation for AA to be applicable to large-scale inference.

Despite offering interpretable results, AA did not gain equal attention compared to its alternatives. One possible reason, as pointed out in [6], is due to the lack of efficient computational resources for applying AA to large-scale datasets, which are becoming increasingly ubiquitous in the big-data era. Indeed, the optimization defined in (1.1) is non-convex, and one common approach to solving (1.1) is based on an alternating minimization algorithm [9], which will be reviewed in Section 2. The subproblems in the alternating minimization scheme are equivalent to quadratic programming, which makes the full loop for solving AA computationally intensive for moderately large dimension d and cardinality N .

The scope of this paper is to provide a promising perspective for addressing the theoretical computational challenges encountered by AA. Instead of focusing on optimizing the subproblem solvers to accelerate computation, we introduce two separate dimensionality reduction techniques to downsize the problem before applying optimization methods to solve (1.1). We show that under appropriate conditions, a solution of the reduced AA (i) well-approximates the solution of the original problem (1.1) in terms of projection error and (ii) can be obtained significantly faster than the original solution. Our approach relies on a few far-reaching results in high-dimensional geometry. Note that our proposed

method is a data preprocessing procedure by nature, and complements the many existing methods to further accelerate computation.

1.1 Related work

Making archetypal analysis practical for large-scale data analysis has been an active area of research in recent years. Various approaches have been proposed to attack the problem from different perspectives. For example, feasible optimization techniques such as projected gradients [29], active-subsets [6], and the Frank-Wolfe method [4] are considered for accelerating solving the quadratic programming in the alternating minimization scheme. Relaxation methods including decoupling [28] and sparse projections [1] are concerned with relaxing the alternating minimization into problems that enjoy better scalability properties. Another direction of work is centered around approximately solving AA by first reducing the cardinality of the data via sparse representation [39, 25]. Although these approaches are demonstrated to work well empirically, they either do not address the intrinsic complexity of the problem or lack theoretical guarantee on the quality of approximation. In recent work [26], the authors proposed to use the coresnet of the data to reduce computational complexity of the objective function and theoretically quantified the approximation error.

Using approximate isometric embedding to reduce dimensionality is a fruitful idea in data analysis. The technique has been successfully applied to a variety of problems including least-squares regression [11, 2], clustering [5, 8, 27], low-rank approximation [41, 7, 17], nonnegative matrix factorization [13, 32], and tensor decomposition [44, 3].

1.2 Contributions of this paper

This paper proposes two novel dimensionality reduction techniques which can be combined with existing approaches to mitigate the inherent complexity of archetypal analysis. Both techniques come with theoretical guarantee on their approximation accuracy. In particular,

- We introduce a data compression technique based on a randomized Krylov subspace method [30] to reduce data dimension. This procedure allows us to circumvent frequent queries to high-dimensional data and is new in the context of archetypal analysis.
- We propose to use random projections to compute an approximate convex hull of the data to reduce the cardinality of the dictionary to represent archetypes.

- We theoretically analyze the approximation accuracy and complexity for both techniques. In particular, we show that the reduced archetypal analysis gives a near-optimal solution but has significantly reduced complexity provided that the data is low-dimensional and approximately described by a few extreme patterns.

Our results yield an approximate algorithm that is capable of dealing with data that is large both in size and dimension. Numerical experiments are provided which support and illustrate our theoretical findings.

1.3 Outline

The rest of the paper is organized as follows. In Section 2, we review the standard alternating minimization algorithm for solving archetypal analysis as well as the corresponding computational challenges. In Section 3 and 4, we introduce two separate randomized techniques to reduce the data dimension and representation cardinality of the archetypes, respectively. We also quantify the approximation accuracy and the computational complexity for both techniques. In Section 5, we combine the ideas in Section 3 and 4 to devise an approximate algorithm for archetypal analysis. We show that the proposed algorithm gives a near-optimal solution meanwhile has significantly reduced computational complexity for datasets that are approximately embedded in a low-dimensional subspace and well summarized via a few extreme points. We numerically verify our results in Section 6.

1.4 Notation

In the rest of the paper, $\mathbf{X} \in \mathbb{R}^{d \times N}$ denotes the data matrix. We always use $(\mathbf{A}_\star, \mathbf{B}_\star)$ to denote a minimizer to (1.1), and $\text{opt}(\mathbf{X}) = \frac{1}{\sqrt{N}} \|\mathbf{X} - \mathbf{X} \mathbf{A}_\star \mathbf{B}_\star\|_F$ the corresponding optimum value.

Denote $[m] = \{1, \dots, m\} \subset \mathbb{N}$. For a matrix $\mathbf{A} \in \mathbb{R}^{m \times n}$, we denote by $\sigma_i(\mathbf{A})$ the i -th largest singular value of \mathbf{A} , and \mathbf{A}^\dagger the Moore-Penrose pseudoinverse of \mathbf{A} . For $T_1 \subset [m]$ and $T_2 \subset [n]$, we use notation $\mathbf{A}[T_1, :]$, $\mathbf{A}[-T_1, :]$, $\mathbf{A}[:, T_2]$, and $\mathbf{A}[:, -T_2]$ to denote the submatrices formed by taking the rows of \mathbf{A} with indices in T_1 , the rows of \mathbf{A} with indices in $[m] \setminus T_1$, the columns of \mathbf{A} with indices in T_2 , and the columns of \mathbf{A} with indices in $[n] \setminus T_2$, respectively. When talking about subspace embedding for \mathbf{A} , we view \mathbf{A} as n points $\mathbf{A}[:, 1], \dots, \mathbf{A}[:, n]$ in the column space of \mathbf{A} , i.e., $\text{col}(\mathbf{A})$. We use $\text{conv}(\mathbf{A})$ and $\text{ex}(\mathbf{A})$ to represent the convex hull of the columns of \mathbf{A} and the corresponding extreme points, respectively.

Moreover, $\mathcal{O}(\cdot)$, $a(n_1, \dots, n_\ell) \lesssim b(n_1, \dots, n_\ell)$ and $a(n_1, \dots, n_\ell) \gtrsim b(n_1, \dots, n_\ell)$ are standard notation in complexity theory, where the implicit constants do not depend on the indices n_1, \dots, n_ℓ .

2 An alternating minimization algorithm for archetypal analysis

In this section, we review an alternating minimization algorithm for solving AA, due to Cutler and Breiman [9]. Note that (1.1) is a non-convex optimization. However, when fixing \mathbf{A} or \mathbf{B} and solving for the other, the problem becomes convex. This observation gives rise to the following alternating minimization algorithm for computing a stationary solution for (1.1).

Algorithm 1: Alternating Minimization Algorithm for AA [9]

Input: $\{x_i\}_{i \in [N]}$: dataset, k : number of archetypes

Output: \mathbf{A}, \mathbf{B}

- 1: Initialize $\mathbf{X}\mathbf{A}$
 - 2: **while** not converged **do**
 - 3: $\mathbf{B} \leftarrow \arg \min_{\mathbf{B}' \in \mathbb{R}_{\text{CS}}^{k \times N}} \|\mathbf{X} - \mathbf{X}\mathbf{A}\mathbf{B}'\|_F^2$
 - 4: $\mathbf{A} \leftarrow \arg \min_{\mathbf{A}' \in \mathbb{R}_{\text{CS}}^{N \times k}} \|\mathbf{X} - \mathbf{X}\mathbf{A}'\mathbf{B}\|_F^2$
 - 5: **end while**
 - 6: final update for \mathbf{B} : $\mathbf{B} \leftarrow \arg \min_{\mathbf{B}' \in \mathbb{R}_{\text{CS}}^{k \times N}} \|\mathbf{X} - \mathbf{X}\mathbf{A}\mathbf{B}'\|_F^2$
 - 7: return \mathbf{A}, \mathbf{B}
-

The loop in Algorithm 1 requires updating \mathbf{B} and \mathbf{A} alternately. To analyze the computational complexity of these subroutines, we formulate the optimization problems in step 3 and 4 more explicitly as follows.

In step 3, \mathbf{A} is fixed and \mathbf{B} needs to be updated. If we let $\mathbf{Z} = \mathbf{X}\mathbf{A}$, then the optimization is equivalent to computing the projection coefficients for each column in \mathbf{X} to $\text{conv}(\mathbf{Z})$. In particular, we need to solve N independent quadratic programming with variable dimension k :

$$\min_{b \in \mathbb{R}^k, \|b\|_1=1, b \geq 0} \|\mathbf{Z}b - x_i\|_2^2 \quad i \in [N].$$

In step 4, \mathbf{B} is fixed and \mathbf{A} , or equivalently, \mathbf{Z} , needs to be updated. In this case, a Gauss-Siedel approach can be used to update the columns of \mathbf{Z} sequentially more efficiently [31] than directly computing \mathbf{Z} at once:

$$\begin{aligned} & \min_{z = \mathbf{X}a \in \mathbb{R}^d, \|a\|_1=1, a \geq 0} \|z - \mathbf{D}_i(\mathbf{B}[i, :])^T / \|\mathbf{B}[i, :]\|_2^2\|_2^2 \\ &= \min_{a \in \mathbb{R}^N, \|a\|_1=1, a \geq 0} \|\mathbf{X}a - \mathbf{D}_i(\mathbf{B}[i, :])^T / \|\mathbf{B}[i, :]\|_2^2\|_2^2 \quad i \in [k], \end{aligned}$$

where $\mathbf{D}_i = \mathbf{X} - \mathbf{Z}[:, -i]\mathbf{B}[-i, :]$. For either method, step 4 involves solving k quadratic programming

with variable dimension N .

For small k and large N , the computation time in step 3 scales linearly in N (assuming solving a k -dimensional quadratic programming takes constant time). For step 4, the computation time is approximately equal to a multiplicative constant (k) times the complexity of solving an N -dimensional quadratic programming, which can be computationally infeasible for large N . We will provide a theoretically justified accelerated scheme for step 4 in Section 4. Moreover, when d is large, taking repeated numerical operations on \mathbf{X} is inconvenient. We will introduce a data dimensionality reduction technique to address this issue in Section 3.

3 Data dimensionality reduction

We first consider the scenario where the data dimension is large. This may happen, for instance, when each data point is obtained from the discretization of a continuous function (time series), or encodes a high-resolution image. In this case, directly working with the data is inconvenient. Instead, we can embed \mathbf{X} in a lower dimensional space while maintaining the convexity structure of \mathbf{X} . This compression will save us from frequently querying the columns of \mathbf{X} in the iterative process for solving (1.1), which can be computationally expensive. A straightforward idea for embedding is via singular value decomposition (SVD), which we recall below:

Definition 3.1. Suppose $d \geq N$, and $\text{rank}(\mathbf{X}) = r \leq N$. The singular value decomposition (SVD) of \mathbf{X} is given by $\mathbf{X} = \mathbf{U}\mathbf{\Sigma}\mathbf{V}^T$, where $\mathbf{U} \in \mathbb{R}^{d \times r}$, $\mathbf{V} \in \mathbb{R}^{r \times N}$ are the left and right singular vector matrices, respectively, and $\mathbf{\Sigma} \in \mathbb{R}^{r \times r}$ is a diagonal matrix with diagonal entries arranged in non-increasing order.

Under the columns of \mathbf{U} , $\mathbf{\Sigma}\mathbf{V}^T \in \mathbb{R}^{r \times N}$ provides a sparse representation for \mathbf{X} (since $r \leq d$). If we first embed \mathbf{X} in \mathbf{U} using SVD and apply AA to $\mathbf{\Sigma}\mathbf{V}^T$, then for every feasible (\mathbf{A}, \mathbf{B}) , by the unitary invariance of Frobenius norm,

$$\|\mathbf{\Sigma}\mathbf{V}^T - \mathbf{\Sigma}\mathbf{V}^T\mathbf{A}\mathbf{B}\|_F^2 = \|\mathbf{U}^T\mathbf{X} - \mathbf{U}^T\mathbf{X}\mathbf{A}\mathbf{B}\|_F^2 = \|\mathbf{X} - \mathbf{X}\mathbf{A}\mathbf{B}\|_F^2, \quad (3.1)$$

which establishes the equivalence between (1.1) and the AA under the SVD representation.

In fact, if \mathbf{X} has full rank but possesses low-rank structure, one may use a truncated SVD to further reduce the data dimension at a minor cost of accuracy, as made precise in the following theorem:

Theorem 3.1. Suppose $p \leq r = \text{rank}(\mathbf{X})$. Denote by $\mathbf{U}_p, \mathbf{V}_p$ the first p columns of \mathbf{U} and \mathbf{V} , respectively, and $\mathbf{\Sigma}_p$ the top $p \times p$ submatrix of $\mathbf{\Sigma}$. Let $(\tilde{\mathbf{A}}, \tilde{\mathbf{B}})$ be a solution to the AA for the truncated SVD

representation of \mathbf{X} at p -th level:

$$\min_{\mathbf{A} \in \mathbb{R}_{cs}^{N \times k}, \mathbf{B} \in \mathbb{R}_{cs}^{k \times N}} \frac{1}{\sqrt{N}} \|\Sigma_p \mathbf{V}_p^T - \Sigma_p \mathbf{V}_p^T \mathbf{A} \mathbf{B}\|_F.$$

Then,

$$\frac{1}{\sqrt{N}} \|\mathbf{X} - \mathbf{X} \tilde{\mathbf{A}} \tilde{\mathbf{B}}\|_F \leq \text{opt}(\mathbf{X}) + 4\sigma_{p+1}(\mathbf{X}). \quad (3.2)$$

Proof. Let

$$\mathbf{X}_p := \mathbf{U}_p \Sigma_p \mathbf{V}_p \quad \mathbf{X}_{-p} := \mathbf{X} - \mathbf{X}_p. \quad (3.3)$$

By the Eckart–Young theorem [12], \mathbf{X}_p is the best rank- p approximation for \mathbf{X} in the spectral norm, with approximation error $\|\mathbf{X}_{-p}\|_2 = \sigma_{p+1}(\mathbf{X})$. Let $(\mathbf{A}_\star, \mathbf{B}_\star)$ be a solution to (1.1). Consequently,

$$\begin{aligned} \|\mathbf{X} - \mathbf{X} \tilde{\mathbf{A}} \tilde{\mathbf{B}}\|_F &\leq \|\mathbf{X}_p - \mathbf{X}_p \tilde{\mathbf{A}} \tilde{\mathbf{B}}\|_F + \|\mathbf{X}_{-p} - \mathbf{X}_{-p} \tilde{\mathbf{A}} \tilde{\mathbf{B}}\|_F \\ &= \|\mathbf{U}_p \Sigma_p \mathbf{V}_p^T - \mathbf{U}_p \Sigma_p \mathbf{V}_p^T \tilde{\mathbf{A}} \tilde{\mathbf{B}}\|_F + \|\mathbf{X}_{-p} - \mathbf{X}_{-p} \tilde{\mathbf{A}} \tilde{\mathbf{B}}\|_F \\ &= \|\Sigma_p \mathbf{V}_p^T - \Sigma_p \mathbf{V}_p^T \tilde{\mathbf{A}} \tilde{\mathbf{B}}\|_F + \|\mathbf{X}_{-p} - \mathbf{X}_{-p} \tilde{\mathbf{A}} \tilde{\mathbf{B}}\|_F \\ &\leq \|\Sigma_p \mathbf{V}_p^T - \Sigma_p \mathbf{V}_p^T \mathbf{A}_\star \mathbf{B}_\star\|_F + \|\mathbf{X}_{-p} - \mathbf{X}_{-p} \tilde{\mathbf{A}} \tilde{\mathbf{B}}\|_F \\ &= \|\mathbf{U}_p \Sigma_p \mathbf{V}_p^T - \mathbf{U}_p \Sigma_p \mathbf{V}_p^T \mathbf{A}_\star \mathbf{B}_\star\|_F + \|\mathbf{X}_{-p} - \mathbf{X}_{-p} \tilde{\mathbf{A}} \tilde{\mathbf{B}}\|_F \\ &= \|\mathbf{X}_p - \mathbf{X}_p \mathbf{A}_\star \mathbf{B}_\star\|_F + \|\mathbf{X}_{-p} - \mathbf{X}_{-p} \tilde{\mathbf{A}} \tilde{\mathbf{B}}\|_F \\ &\leq \|\mathbf{X} - \mathbf{X} \mathbf{A}_\star \mathbf{B}_\star\|_F + \|\mathbf{X}_{-p} - \mathbf{X}_{-p} \mathbf{A}_\star \mathbf{B}_\star\|_F + \|\mathbf{X}_{-p} - \mathbf{X}_{-p} \tilde{\mathbf{A}} \tilde{\mathbf{B}}\|_F \\ &\leq \|\mathbf{X} - \mathbf{X} \mathbf{A}_\star \mathbf{B}_\star\|_F + 2\|\mathbf{X}_{-p}\|_F + \|\mathbf{X}_{-p} \mathbf{A}_\star \mathbf{B}_\star\|_F + \|\mathbf{X}_{-p} \tilde{\mathbf{A}} \tilde{\mathbf{B}}\|_F. \end{aligned} \quad (3.4)$$

Since $\mathbf{A}_\star, \tilde{\mathbf{A}}, \mathbf{B}_\star, \tilde{\mathbf{B}}$ are column stochastic matrices, $\mathbf{A}_\star \mathbf{B}_\star$ and $\tilde{\mathbf{A}} \tilde{\mathbf{B}}$ are also column stochastic matrices.

It follows from direct computation and the Cauchy-Schwarz inequality that

$$\begin{aligned} \|\mathbf{X}_{-p} \mathbf{A}_\star \mathbf{B}_\star\|_F &= \sqrt{\sum_{i \in [N]} \|\mathbf{X}_{-p}(\mathbf{A}_\star \mathbf{B}_\star)[\cdot, i]\|_2^2} \leq \sqrt{\sum_{i \in [N]} \|\mathbf{X}_{-p}\|_2^2 \|(\mathbf{A}_\star \mathbf{B}_\star)[\cdot, i]\|_2^2} \\ &\leq \sqrt{\sum_{i \in [N]} \|\mathbf{X}_{-p}\|_2^2 \|(\mathbf{A}_\star \mathbf{B}_\star)[\cdot, i]\|_1^2} \\ &\leq \|\mathbf{X}_{-p}\|_2 \sqrt{N}. \end{aligned} \quad (3.5)$$

Similarly,

$$\|\mathbf{X}_{-p}\widetilde{\mathbf{A}}\widetilde{\mathbf{B}}\|_F \leq \|\mathbf{X}_{-p}\|_2\sqrt{N}. \quad (3.6)$$

Plugging (3.5) and (3.6) into (3.4) and dividing by \sqrt{N} yields

$$\begin{aligned} \frac{1}{\sqrt{N}}\|\mathbf{X} - \mathbf{X}\widetilde{\mathbf{A}}\widetilde{\mathbf{B}}\|_F &\leq \text{opt}(\mathbf{X}) + \frac{2}{\sqrt{N}}\|\mathbf{X}_{-p}\|_F + 2\|\mathbf{X}_{-p}\|_2 \leq \text{opt}(\mathbf{X}) + 4\|\mathbf{X}_{-p}\|_2 \\ &= \text{opt}(\mathbf{X}) + 4\sigma_{p+1}(\mathbf{X}), \end{aligned}$$

completing the proof. \square

Thus, for data \mathbf{X} that admits a good low-rank approximation, AA applied to the truncated SVD representation yields a near-optimal solution in terms of prediction errors. In this case, the data dimension can be significantly reduced to streamline computation. However, to obtain truncated SVD representations, one often needs to compute the full SVD of \mathbf{X} , which has complexity $\mathcal{O}(dN \min\{d, N\})$. For large d and N , this procedure is computationally intensive and thus can be restrictive in practice. To address this issue, we consider an approximate version of the best rank- p approximation without taking the SVD of \mathbf{X} .

Definition 3.2. A matrix $\widetilde{\mathbf{X}}_p$ is a $(1 + \varepsilon)$ rank- p approximation to \mathbf{X} if $\text{rank}(\widetilde{\mathbf{X}}_p) \leq p$ and

$$\|\mathbf{X} - \widetilde{\mathbf{X}}_p\|_2 \leq (1 + \varepsilon)\|\mathbf{X} - \mathbf{X}_p\|_2, \quad (3.7)$$

where \mathbf{X}_p is the best rank- p approximation to \mathbf{X} as defined in (3.3).

Before turning to discuss how to find such an $\widetilde{\mathbf{X}}_p$, we consider a few consequences assuming its existence. Similar to the previous discussion, we can apply AA to $\widetilde{\mathbf{X}}_p$, which can be efficiently represented using the SVD. As will be seen shortly, computing the SVD of $\widetilde{\mathbf{X}}_p$ is much cheaper than \mathbf{X} when p is small. On the other hand, let $\widetilde{\mathbf{X}}_p = \widetilde{\mathbf{U}}_p \widetilde{\boldsymbol{\Sigma}}_p \widetilde{\mathbf{V}}_p^T$ be the SVD of $\widetilde{\mathbf{X}}_p$ and define

$$\widetilde{\mathbf{X}} = \widetilde{\boldsymbol{\Sigma}}_p \widetilde{\mathbf{V}}_p^T \implies \widetilde{\mathbf{X}}_p = \widetilde{\mathbf{U}}_p \widetilde{\mathbf{X}}.$$

The following theorem quantifies the approximation error if we use $\widetilde{\mathbf{X}}$ in place of \mathbf{X} for archetypal analysis:

Theorem 3.2. Let $\varepsilon > 0$. Suppose $\widetilde{\mathbf{X}}_p$ is a $(1 + \varepsilon)$ rank- p approximation to \mathbf{X} , and $\widetilde{\mathbf{X}}$ is the representation of $\widetilde{\mathbf{X}}_p$ under the left singular vectors. Let $(\widetilde{\mathbf{A}}, \widetilde{\mathbf{B}})$ be a solution to the AA applied to $\widetilde{\mathbf{X}}$:

$$\min_{\mathbf{A} \in \mathbb{R}_{cs}^{N \times k}, \mathbf{B} \in \mathbb{R}_{cs}^{k \times N}} \frac{1}{\sqrt{N}} \left\| \widetilde{\mathbf{X}} - \widetilde{\mathbf{X}} \mathbf{A} \mathbf{B} \right\|_F. \quad (3.8)$$

Then,

$$\frac{1}{\sqrt{N}} \left\| \mathbf{X} - \mathbf{X} \widetilde{\mathbf{A}} \widetilde{\mathbf{B}} \right\|_F \leq \text{opt}(\mathbf{X}) + 4(1 + \varepsilon) \sigma_{p+1}(\mathbf{X}).$$

Proof. Proceeding similarly as proof of Theorem 3.1 with $\mathbf{X}_p, \mathbf{X}_{-p}$ replaced by $\widetilde{\mathbf{X}}_p$ and $\widetilde{\mathbf{X}}_{-p} = \mathbf{X} - \widetilde{\mathbf{X}}_p$, respectively,

$$\frac{1}{\sqrt{N}} \left\| \mathbf{X} - \mathbf{X} \widetilde{\mathbf{A}} \widetilde{\mathbf{B}} \right\|_F \leq \text{opt}(\mathbf{X}) + 4 \left\| \widetilde{\mathbf{X}}_{-p} \right\|_2 \stackrel{(3.7)}{\leq} \text{opt}(\mathbf{X}) + 4(1 + \varepsilon) \sigma_{p+1}(\mathbf{X}).$$

□

Theorem 3.2 implies that for \mathbf{X} with small best rank- p approximation error, using the SVD representation of $\widetilde{\mathbf{X}}_p$ will only result in a small impact on prediction accuracy. The following result, due to Musco and Musco [30], shows that $\widetilde{\mathbf{X}}_p$ (i.e., $\widetilde{\mathbf{X}}$) can be efficiently computed via randomized block Krylov methods. The details of the algorithm are given in Algorithm 2:

Algorithm 2: Block Krylov Iteration [30]

Input: $\mathbf{X} \in \mathbb{R}^{d \times N}$: data matrix, p : approximation rank, s : power parameter

Output: $\widetilde{\mathbf{X}}_p$

- 1: generate p random initializations: $\mathbf{S} \in \mathbb{R}^{N \times p}$, $\mathbf{S}_{ij} \stackrel{\text{i.i.d}}{\sim} \mathcal{N}(0, 1)$
 - 2: construct the Krylov subspace: $\mathbf{K} = [\mathbf{X} \mathbf{S}, (\mathbf{X} \mathbf{X}^T) \mathbf{X} \mathbf{S}, \dots, (\mathbf{X} \mathbf{X}^T)^{s-1} \mathbf{X} \mathbf{S}] \in \mathbb{R}^{d \times (sp)}$
 - 3: compute the QR decomposition for \mathbf{K} : $\mathbf{K} = \mathbf{Q} \mathbf{R}$
 - 4: compute the SVD of $\mathbf{X}_{\text{emd}} = \mathbf{X}^T \mathbf{Q}$: $\mathbf{X}_{\text{emd}} = \mathbf{U}_{\text{emd}} \boldsymbol{\Sigma}_{\text{emd}} \mathbf{V}_{\text{emd}}^T$
 - 5: compute $\widetilde{\mathbf{X}}$: $\widetilde{\mathbf{X}}_p = \mathbf{L} \mathbf{L}^T \mathbf{X}$, with $\mathbf{L} = \mathbf{Q} \mathbf{V}_{\text{emd}}[:, 1 : p]$
-

It was established in [30] that for reasonably large s , with high probability, $\widetilde{\mathbf{X}}_p$ returned by Algorithm 2 is a good approximation to \mathbf{X}_p . Before providing the precise result in Lemma 3.1, we digress for the moment to discuss the computation of $\widetilde{\mathbf{X}}$.

Note that to apply Theorem 3.2, we need to compute the SVD representation of $\widetilde{\mathbf{X}}_p$ (i.e., $\widetilde{\mathbf{X}}$) rather than itself. This additional step may incur additional computational cost for general $\widetilde{\mathbf{X}}_p$. However, in

our case, $\widetilde{\mathbf{X}}$ can be obtained off the shelf.

Theorem 3.3. *Let $\widetilde{\mathbf{X}}$ be the SVD representation of $\widetilde{\mathbf{X}}_p$ in Algorithm 2. Then, the computational complexity for $\widetilde{\mathbf{X}}_p$ is $\mathcal{O}(dNps + \max\{d, N\}(ps)^2)$.*

Proof. Denote the SVD of $\mathbf{L}^T \mathbf{X}$ as

$$\mathbf{L}^T \mathbf{X} = \widehat{\mathbf{U}}_p \widehat{\boldsymbol{\Sigma}}_p \widehat{\mathbf{V}}_p^T. \quad (3.9)$$

Since \mathbf{L} has orthonormal columns, the SVD representation of $\widetilde{\mathbf{X}}_p$ is the same as that for $\mathbf{L}^T \mathbf{X}$:

$$\widetilde{\mathbf{X}} = \widehat{\boldsymbol{\Sigma}}_p \widehat{\mathbf{V}}_p^T, \quad (3.10)$$

with left singular matrix given by

$$\widetilde{\mathbf{U}}_p = \mathbf{L} \widehat{\mathbf{U}}_p. \quad (3.11)$$

On the other hand, the SVD of $\mathbf{L}^T \mathbf{X}$ can be easily found using computed components in step 4 in Algorithm 2:

$$\begin{aligned} \mathbf{L}^T \mathbf{X} &= (\mathbf{V}_{\text{emd}}[:, 1:p])^T \mathbf{Q}^T \mathbf{X} = (\mathbf{V}_{\text{emd}}[:, 1:p])^T \mathbf{V}_{\text{emd}} \boldsymbol{\Sigma}_{\text{emd}} \mathbf{U}_{\text{emd}}^T \\ &= \mathbf{I}_p \boldsymbol{\Sigma}_{\text{emd}}[1:p, 1:p] (\mathbf{U}_{\text{emd}}[:, 1:p])^T, \end{aligned}$$

i.e.,

$$\widetilde{\mathbf{X}} = \boldsymbol{\Sigma}_{\text{emd}}[1:p, 1:p] (\mathbf{U}_{\text{emd}}[:, 1:p])^T. \quad (3.12)$$

Thus, the computational complexity of $\widetilde{\mathbf{X}}$ can be obtained by computing the running time of Algorithm 2 up to step 4. Step 1 generates a random Gaussian matrix which takes time $\mathcal{O}(Np)$. Step 2 involves computation of Krylov subspace basis. If we compute the i -th block using information from the previous block: $(\mathbf{X} \mathbf{X}^T)^i \mathbf{X} \mathbf{S} = \mathbf{X} [\mathbf{X}^T ((\mathbf{X} \mathbf{X}^T)^{i-1} \mathbf{X} \mathbf{S})]$, then the whole step takes time $\mathcal{O}(dNps)$. The QR decomposition of \mathbf{K} in step 3 costs time $\mathcal{O}(ds^2p^2)$. In step 4, we first compute \mathbf{X}_{emd} , which takes time $\mathcal{O}(dNps)$, then compute the SVD of \mathbf{X}_{emd} , which takes time $\mathcal{O}(Nps \cdot \min\{N, ps\})$. The proof is finished by putting the times together. \square

Remark 3.1. When $sp \ll \min\{d, N\}$, the computational complexity of $\widetilde{\mathbf{X}}_p$ becomes $\mathcal{O}(dNps)$, which is

significantly smaller than $\mathcal{O}(dN \min\{d, N\})$.

To get some intuition why the $\widetilde{\mathbf{X}}_p$ in Algorithm 2 almost matches the best rank- p approximation \mathbf{X}_p in the spectral norm, we will recall a few well used results in numerical linear algebra. The best rank- p approximation \mathbf{X}_p is obtained by projecting the columns of \mathbf{X} to the subspace spanned by the first p left singular vectors of \mathbf{X} : $\mathbf{X}_p = \mathbf{U}_p \mathbf{U}_p^T \mathbf{X}$. Thus, our quest for $\widetilde{\mathbf{X}}_p$ boils down to seeking a p -dimensional subspace \mathbf{L} (in the column space of \mathbf{X}) that is ‘close’ to \mathbf{U}_p .

Directly finding such an \mathbf{L} is almost as hard as finding \mathbf{X}_p . Alternatively, one can first find a slightly larger subspace $\widetilde{\mathbf{L}}$, which can be effectively constructed using ideas of oblivious sketching [45]. In this case, $\widetilde{\mathbf{L}}$ is taken as a randomly selected subspace so that the columns of $\widetilde{\mathbf{L}}$ contain the information of \mathbf{U}_p in a uniform way. When the dimension of $\widetilde{\mathbf{L}}$ is sufficiently large, say $\mathcal{O}(p/\varepsilon)$, with high probability, \mathbf{U}_p and $\widetilde{\mathbf{L}}$ are well aligned, so that the projection of \mathbf{U}_p to $\widetilde{\mathbf{L}}$ provides a good candidate for \mathbf{L} . However, as \mathbf{U}_p is unknown, the projection is not explicitly computable, but one can get around this by taking SVD of $\widetilde{\mathbf{L}}^T \mathbf{X}$ to yield a desired rank approximation. Such a procedure is shown to produce a low-rank matrix that enjoys similar approximation accuracy as (3.7) but under the Frobenius norm [37, 45].

In general, an error bound in the Frobenius norm does not imply a similar bound in the spectral norm, unless the singular values of \mathbf{X} have fast-decaying properties. Since \mathbf{X} and $(\mathbf{X}\mathbf{X}^T)^s \mathbf{X}$ have the same singular vectors for any $s \in \mathbb{N}$, i.e., $(\mathbf{X}\mathbf{X}^T)^s \mathbf{X} = \mathbf{U}_p \Sigma^{2s+1} \mathbf{V}^T$, while the singular values of the latter are much more spread when s is large, this suggests the possibility of working with $(\mathbf{X}\mathbf{X}^T)^s \mathbf{X}$ to find an \mathbf{L} to meet (3.7). This is nothing but a randomized version of the simultaneous iteration method in classical numerical linear algebra [36, 40].

When applying sketching to $(\mathbf{X}\mathbf{X}^T)^s \mathbf{X}$, the initial randomness in $\widetilde{\mathbf{L}}$ (the dimension of $\widetilde{\mathbf{L}}$) can be reduced to p thanks to the amplifying effect of powering. Indeed, as long as the columns of \mathbf{U}_p are not orthogonal to $\widetilde{\mathbf{L}}$ (which is the purpose of randomization), $(\mathbf{X}\mathbf{X}^T)^s \mathbf{X} \widetilde{\mathbf{L}}$ nearly coincides with \mathbf{U}_p for large s , and can be used as a good candidate for \mathbf{L} [34, 17, 45]. Algorithm 2, at large, is similar to the randomized simultaneous iteration approach, but utilizes a more efficient polynomial of \mathbf{X} than \mathbf{X}^s for spectral separation. In fact, one only needs such a polynomial to exist to ensure a good approximation, which in practice is alternatively computed via a projected SVD as before. The next lemma summarizes the above procedure in a qualitative statement:

Lemma 3.1 ([30]). *For $\varepsilon, \delta > 0$, there exist absolute constants $C_1, C_2 > 0$ such that if*

$$s > \frac{C_1}{\sqrt{\varepsilon}} \log \left(\frac{N}{\varepsilon \delta} \right) \qquad p \geq C_2 \log \left(\frac{4}{\delta} \right), \qquad (3.13)$$

then for with probability at least $1 - \delta$, the $\widetilde{\mathbf{X}}_p$ in Algorithm 2 satisfies (3.7).

Remark 3.2. Lemma 3.1 is a probabilistic version of [30, Theorem 1] where a fixed probability (0.99) is used instead of $1 - \delta$ for an arbitrary δ . Nevertheless, the proof is the same except one needs to apply sharp concentration inequalities to bound extreme singular values of Gaussian matrices [43, Corollary 7.3.3], [35, Theorem 1.2] to bound the failing probability.

Setting $\varepsilon = 1$ in Lemma 3.1 and combining Theorem 3.2, we have the following result:

Theorem 3.4. Let $\widetilde{\mathbf{X}}$ (defined in (3.12)) be the SVD representation of $\widetilde{\mathbf{X}}_p$ returned by Algorithm 2. Let $(\widetilde{\mathbf{A}}, \widetilde{\mathbf{B}})$ be a solution to the AA for $\widetilde{\mathbf{X}}$:

$$\min_{\mathbf{A} \in \mathbb{R}_{cs}^{N \times k}, \mathbf{B} \in \mathbb{R}_{cs}^{k \times N}} \frac{1}{\sqrt{N}} \|\widetilde{\mathbf{X}} - \widetilde{\mathbf{X}}\mathbf{A}\mathbf{B}\|_F. \quad (3.14)$$

For $\delta > 0$, if p satisfies (3.13) and $s > C \log(N/\delta)$ for some absolute constant $C > 0$, then with probability at least $1 - \delta$,

$$\frac{1}{\sqrt{N}} \|\mathbf{X} - \mathbf{X}\widetilde{\mathbf{A}}\widetilde{\mathbf{B}}\|_F \leq \text{opt}(\mathbf{X}) + 8\sigma_{p+1}(\mathbf{X}).$$

Remark 3.3. Fixing δ small, say $\delta = 0.01$, $s = \mathcal{O}(\log N)$. The computational complexity of $\widetilde{\mathbf{X}}$ is $\mathcal{O}(dNp \log N + \max\{d, N\} \log^2 Np^2)$. Consequently, for data \mathbf{X} that can be well approximated via low-rank matrices with approximation rank $p \ll N$, using Algorithm 2 can effectively reduce the dimension of AA.

4 Representation cardinality reduction

We now consider the situation where the dataset has a large cardinality, i.e., $N > d$. In this case, to reduce computational complexity, we propose to use a parsimonious subset of points in \mathbf{X} to approximately represent $\text{conv}(\mathbf{X})$, i.e., we wish to find a small subset $T \subset [N]$ such that

$$\text{conv}(\mathbf{X}_T) \approx \text{conv}(\mathbf{X}), \quad (4.1)$$

where $\mathbf{X}_T := \mathbf{X}[:, T]$ and \approx will be made rigorous later. We will refer to $\text{conv}(\mathbf{X}_T)$ as an *approximate convex hull* of \mathbf{X} .

The idea of using subsets of \mathbf{X} (i.e. extreme points) to represent $\text{conv}(\mathbf{X})$ has been considered in

[39, 25], where exact equality in (4.1) is expected. Here we only ask for approximate representation of $\text{conv}(\mathbf{X})$ (allowing for a small approximation error), so that it is possible to further reduce the cardinality of the representation set for the archetypes (Figure 1).

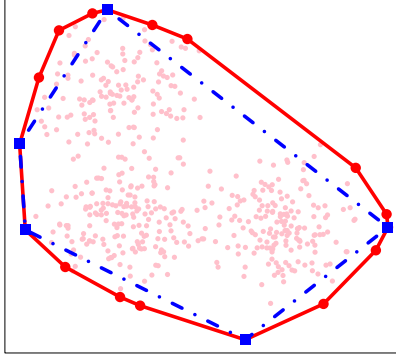


Figure 1: An example of the convex hull (red solid curves) and an approximate convex hull (blue dashed curve) of a randomly generated dataset.

Similar to the discussion in the previous section, we first give a few consequences assuming \mathbf{X}_T exists.

Definition 4.1. We say that \mathbf{X}_T is an ε -approximate convex hull of \mathbf{X} if

$$d_H(\text{conv}(\mathbf{X}_T), \text{conv}(\mathbf{X})) \leq \varepsilon, \quad (4.2)$$

where $d_H(X, Y) := \max \{ \sup_{x \in X} d(x, Y), \sup_{y \in Y} d(X, y) \}$ is the Hausdorff distance.

Theorem 4.1. For $\varepsilon > 0$ and $T \subset [N]$, suppose \mathbf{X}_T is a $(\text{opt}(\mathbf{X}) \cdot \varepsilon)$ -approximate convex hull of \mathbf{X} . Consider the following AA optimization problem constrained to $\text{conv}(\mathbf{X}_T)$:

$$\min_{\mathbf{A} \in \mathbb{R}_{cs}^{|T| \times k}, \mathbf{B} \in \mathbb{R}_{cs}^{k \times N}} \frac{1}{\sqrt{N}} \|\mathbf{X} - \mathbf{X}_T \mathbf{A} \mathbf{B}\|_F. \quad (4.3)$$

Then, the archetype points given by the solution of (4.3) provide a $(1 + \varepsilon)$ -approximation to the solution for (1.1) in terms of prediction errors:

$$\min_{\mathbf{A} \in \mathbb{R}_{cs}^{|T| \times k}, \mathbf{B} \in \mathbb{R}_{cs}^{k \times N}} \frac{1}{\sqrt{N}} \|\mathbf{X} - \mathbf{X}_T \mathbf{A} \mathbf{B}\|_F \leq (1 + \varepsilon) \text{opt}(\mathbf{X}).$$

Proof. For an optimal solution $(\mathbf{A}_*, \mathbf{B}_*)$ of (1.1) that resides on the boundary of $\text{conv}(\mathbf{X})$ (such a solution

always exists [9]), consider the projection of each column of $\mathbf{X}\mathbf{A}_\star$ to $\text{conv}(\mathbf{X}_T)$, and denote the projected points as \mathbf{Z} . Note that \mathbf{Z} is well-defined as $\text{conv}(\mathbf{X}_T) \subset \text{conv}(\mathbf{X})$. By the triangle inequality, the distance between each column of \mathbf{X} and $\text{conv}(\mathbf{Z})$ is bounded by the sum of the distance between the column of \mathbf{X} and $\text{conv}(\mathbf{X}\mathbf{A}_\star)$ and $d_H(\mathbf{X}\mathbf{A}_\star, \mathbf{Z})$. Since \mathbf{X}_T gives an $(\text{opt}(\mathbf{X}) \cdot \varepsilon)$ -approximate convex hull of \mathbf{X} ,

$$d_H(\mathbf{X}\mathbf{A}_\star, \mathbf{Z}) \leq d_H(\text{conv}(\mathbf{X}), \text{conv}(\mathbf{X}_T)) \leq \varepsilon \cdot \text{opt}(\mathbf{X}) = \frac{\varepsilon}{\sqrt{N}} \|\mathbf{X} - \mathbf{X}\mathbf{A}_\star\mathbf{B}_\star\|_F. \quad (4.4)$$

It follows from direct computation that

$$\begin{aligned} \min_{\mathbf{A} \in \mathbb{R}_{\text{cs}}^{|T| \times k}, \mathbf{B} \in \mathbb{R}_{\text{cs}}^{k \times N}} \frac{1}{N} \|\mathbf{X} - \mathbf{X}_T \mathbf{A} \mathbf{B}\|_F^2 &\leq \min_{\mathbf{B} \in \mathbb{R}_{\text{cs}}^{k \times N}} \frac{1}{N} \|\mathbf{X} - \mathbf{Z} \mathbf{B}\|_F^2 \\ &= \frac{1}{N} \sum_{i \in [N]} d(x_i, \text{conv}(\mathbf{Z}))^2 \\ &\leq \frac{1}{N} \sum_{i \in [N]} (d(x_i, \text{conv}(\mathbf{X}\mathbf{A}_\star)) + d_H(\mathbf{X}\mathbf{A}_\star, \mathbf{Z}))^2 \\ &\leq (1 + \varepsilon)^2 \cdot \frac{1}{N} \|\mathbf{X} - \mathbf{X}\mathbf{A}_\star\mathbf{B}_\star\|_F^2, \end{aligned}$$

where the last inequality follows from (4.4) and the Cauchy-Schwarz inequality. Taking the square root on both sides completes the proof. \square

Theorem 4.1 establishes an approximate equivalence between the solutions of (4.3) and (1.1) in terms of objective values. Compared to (1.1), the dimension of \mathbf{A} is significantly reduced provided $|T| \ll N$, while the dimension of \mathbf{B} stays unchanged.

To see the computational gain from solving (4.3) instead of (1.1), recall the alternating minimization in Section 2. When \mathbf{B} is fixed and \mathbf{A} is updated, one needs to solve k quadratic programming problems with variable dimension equal to the number of rows of \mathbf{A} . For certain optimization methods such as the ellipsoid method, the complexity of quadratic programming with positive-definite quadratic matrix has weakly polynomial time (of the variable dimension) [23]. Thus, when $|T| \ll N$, a notable acceleration is expected for the subroutine of updating \mathbf{A} , which justifies the significance of using a parsimonious subset of points to represent the archetypes.

On the other hand, when \mathbf{A} is fixed and \mathbf{B} is updated, one needs to compute the projection of each column of \mathbf{X} to $\text{conv}(\mathbf{X}\mathbf{A})$. This step is the same in both (1.1) and (4.3), and consists of N independent quadratic programming problems with variable dimension k . In this case, it is possible to take an additional step of acceleration via parallelization combined with the coresets approximation

[26], which reduces the computation of N projection coefficient vectors to a small subset of points in \mathbf{X} with appropriate weights, similar to the ideas of quadrature. Indeed, given a coreset $\mathbf{X}_C \subset \mathbf{X}$ and appropriate weight diagonal matrix \mathbf{W} , one can approximate the objective function in (1.1) with $\frac{1}{\sqrt{N}} \|\mathbf{W}\mathbf{X}_C - \mathbf{W}\mathbf{X}\mathbf{A}\mathbf{B}\|_F$. Note the complexity of the subproblem for updating \mathbf{B} in the alternating minimization algorithm is proportional to the number of points in the objective function. Therefore, when $|\mathbf{X}_C| \ll |\mathbf{X}|$, the step of solving the \mathbf{B} -subproblem can be significantly accelerated. Combining the idea of coreset with (4.4) yields an approximate objective function $\frac{1}{\sqrt{N}} \|\mathbf{W}\mathbf{X}_C - \mathbf{W}\mathbf{X}_T\mathbf{A}\mathbf{B}\|_F$, which has significantly reduced complexity when solved by the alternating minimization algorithm. The details are not discussed here.

We next discuss how to find a ‘small’ subset T such that (4.2) is satisfied. Note that in order to represent $\text{conv}(\mathbf{X})$, it suffices to consider the extreme points of \mathbf{X} . In other words, we will find a subset $\mathbf{X}_T \subset \text{ex}(\mathbf{X})$ whose convex hull can well approximate $\text{conv}(\mathbf{X})$. As will be seen below, this procedure can be effectively implemented by taking random projections. Indeed, random projections are linear maps whose inverse image of the extreme points of a convex set are a subset of the extreme points of the inverse image of that convex set [24]. Similar ideas have been used in the empirical study of archetypal analysis to seek extreme points [39, 10].

Finding all the extreme points of $\text{conv}(\mathbf{X})$ may itself be computationally demanding unless $\text{ex}(\mathbf{X})$ is small. When $\text{conv}(\mathbf{X})$ can be well approximately using a few extreme points, it is desired to single them out to further shrink the complexity of the problem at small sacrifice of accuracy. To this end, we need to know which extreme points are more important than the others in terms of composing $\text{conv}(\mathbf{X})$. The following result, which originally appeared in [16], is precisely what is needed here.

Observe that under a random projection $v \in \mathbb{S}^{d-1}$, the points in \mathbf{X} have projected values $\{\langle x_i, v \rangle\}_{i \in [N]}$, which with probability one have a unique maximum. The inverse image of the maximum is an element in $\text{ex}(\mathbf{X})$. Thus, throwing away a null set, we can partition the unit sphere \mathbb{S}^{d-1} as follows:

$$\mathbb{S}^{d-1} = \bigsqcup_{x \in \text{ex}(\mathbf{X})} V_x \quad V_x = \{v \in \mathbb{S}^{d-1} : v^T x \geq v^T x_i, i \in [N]\}.$$

For $x \in \text{ex}(\mathbf{X})$, its curvature is defined as

$$\kappa(x) = \frac{|V_x|}{|\mathbb{S}^{d-1}|},$$

which is the relative area of the directions that distinguish x as the maximum to the unit sphere in \mathbb{R}^d .

By definition, points with larger curvature are more likely to be sampled if v is uniformly drawn from \mathbb{S}^{d-1} ; in fact, they are also more ‘important’ as specified by the following lemma [16, Theorem 3.4]:

Lemma 4.1. *Let $S \subset [N]$. Suppose that both $\text{conv}(\mathbf{X}_S)$ and $\text{conv}(\mathbf{X})$ are non-degenerate (i.e., with nonempty interior), and $R := \max_{i \in [N]} \|x_i\|_2$. Then,*

$$d_H(\text{conv}(\mathbf{X}), \text{conv}(\mathbf{X}_S)) \leq \min \left\{ \sqrt{2\pi} (2\omega)^{\frac{1}{d-1}}, 2 \right\} \cdot R \quad \omega = \sum_{i \in [N] \setminus S} \kappa(x_i). \quad (4.5)$$

As a result, to compute a sparse approximate convex hull, it suffices to use high-curvature points to approximately represent $\text{conv}(\mathbf{X})$. To find high-curvature points, one could apply a Monte-Carlo procedure to estimate the curvature of each point, and then truncate based on a given thresholding parameter [16]. To facilitate parsimony, we consider an alternative algorithm that uses a different truncation rule based on ordered cumulative sum. The details are given in Algorithm 3:

Algorithm 3: Approximate Convex Hull

Input: $\{x_i\}_{i \in [N]}$: dataset, M : number of projections, η : approximation accuracy

Output: approximate convex hull $\text{conv}(\{x_i\}_{i \in T})$

- 1: $e_j = 0$ for $j \in [N]$.
 - 2: **for** $i = 1, \dots, M$ **do**
 - 3: $v_i \sim \text{Uniform}(\mathbb{S}^{d-1})$
 - 4: $u_i = \arg \max_j v_i^T x_j$
 - 5: $e_{u_i} \leftarrow e_{u_i} + 1$
 - 6: **end for**
 - 7: sort $\{e_j\}_{j \in [N]}$ in decreasing order as $e^{(1)} \geq \dots \geq e^{(N)}$
 - 8: compute $L = \min \left\{ \ell : \frac{1}{M} \sum_{j \in [\ell]} e^{(j)} > 1 - \eta/3 \right\}$
 - 9: compute $L \leftarrow \max \{L, d + 1\}$
 - 10: let T be the index set of $e^{(1)}, \dots, e^{(L)}$ and return $\{x_j\}_{j \in T}$
-

The computational complexity of Algorithm 3 can be easily obtained from direct computation:

Theorem 4.2. *The computational complexity for Algorithm 3 is $\mathcal{O}(MN(d + \log N))$.*

Proof. The Monte-Carlo procedure in Algorithm 3 (step 2 to 6) involves M repetition of N d -dimensional vector inner product and a sorting. If we apply quicksort [19] for the latter, then the total running time is $\mathcal{O}(M(dN + N \log N))$. Step 7 is a simple sorting which has complexity $\mathcal{O}(N \log N)$. \square

We will show that for large M , with high probability, the output of Algorithm 3 satisfies (4.2) with

$\varepsilon = \min \left\{ \sqrt{2\pi\eta^{\frac{1}{d-1}}}, 2 \right\} \cdot R$. Without loss of generality, in the following discussion we assume $|\text{ex}(\mathbf{X})| = h$ and

$$\kappa(x_1) \geq \kappa(x_2) \geq \cdots \geq \kappa(x_h) > \kappa(x_{h+1}) = \cdots = \kappa(x_N) = 0. \quad (4.6)$$

We have the following theorem:

Theorem 4.3. *Let T be the subset returned by Algorithm 3, and $R = \max_{i \in [N]} \|x_i\|_2$. Suppose $\text{conv}(\mathbf{X}_D)$ is non-degenerate for every $D \subset [N]$ with $|D| > d$. Denote q as the smallest integer such that $\sum_{i \in [q]} \kappa(x_i) \geq 1 - \eta/18$:*

$$q := \min \left\{ j : \sum_{i \in [j]} \kappa(x_i) \geq 1 - \frac{\eta}{18} \right\}, \quad (4.7)$$

and the truncation gap

$$\Delta := \kappa(x_q) - \kappa(x_{q+1}) > 0.$$

If

$$M \geq \max \left\{ \frac{324q^2}{\eta^2}, \frac{4}{\Delta^2} \right\} \log \left(\frac{3N}{\sqrt{\delta}} \right), \quad (4.8)$$

then with probability at least $1 - \delta$, $|T| \leq \max\{q, d + 1\}$ and

$$d_H(\text{conv}(\mathbf{X}_T), \text{conv}(\mathbf{X})) \leq \min \left\{ \sqrt{2\pi\eta^{\frac{1}{d-1}}}, 2 \right\} \cdot R. \quad (4.9)$$

Remark 4.1. Setting the upper bound in (4.9) equal to $\text{opt}(\mathbf{X})\varepsilon$ yields

$$M \geq \max \left\{ 324q^2 \left(\frac{2\pi^2 R^2}{\text{opt}(\mathbf{X})^2 \varepsilon^2} \right)^{d-1}, \frac{4}{\Delta^2} \right\} \log \left(\frac{3N}{\sqrt{\delta}} \right),$$

which has an unpleasant but expected exponential dependence on d (curse of dimensionality). For datasets with low-dimensional structure, i.e., well approximated via rank- p matrices with $p \ll d$, it is possible to use ideas in Section 3 to improve the exponential dimension dependence to p (Algorithm 4).

Proof of Theorem 4.3. Note that step 9 in Algorithm 3 ensures that $\text{conv}(\mathbf{X}_T)$ is non-degenerate. Therefore, to show (4.9), by (4.5), it suffices to show $\sum_{i \in [N] \setminus T} \kappa(x_i) \leq \eta/2$, or equivalently, $\sum_{i \in T} \kappa(x_i) \geq$

$1 - \eta/2$.

We first show that for M satisfying (4.8), with high probability, the estimated curvatures e_j/M are close to their expectations for all reasonably large e_j . Note for every $j \in [q]$, e_j is a sum of M independent Bernoulli random variables with parameter $\kappa(x_j)$, and the tail sum $\sum_{j>q} e_j$ is a sum of M independent Bernoulli random variables with parameter $\sum_{j>q} \kappa(x_j) < \eta/18$. Thus, by Hoeffding's inequality [20],

$$\begin{aligned} \mathbb{P} \left[\left| \frac{1}{M} e_j - \kappa(x_j) \right| \leq \frac{\eta}{18q} \right] &\geq 1 - 2 \exp \left(-\frac{M\eta^2}{162q^2} \right) \\ \mathbb{P} \left[\left| \frac{1}{M} \sum_{j>q} e_j - \sum_{j>q} \kappa(x_j) \right| \leq \frac{\eta}{18q} \right] &\geq 1 - 2 \exp \left(-\frac{M\eta^2}{162q^2} \right). \end{aligned}$$

Taking a union bound over $j \in [q]$ and combining the two inequalities yields

$$\begin{aligned} \mathbb{P} \left[\left\{ \max_{j \in [q]} \left| \frac{1}{M} e_j - \kappa(x_j) \right|, \left| \frac{1}{M} \sum_{j>q} e_j - \sum_{j>q} \kappa(x_j) \right| \right\} \leq \frac{\eta}{18q} \right] \\ \geq 1 - 2(q+1) \exp \left(-\frac{M\eta^2}{162q^2} \right) \geq 1 - 4q \exp \left(-\frac{M\eta^2}{162q^2} \right). \end{aligned} \quad (4.10)$$

The right-hand side in (4.10) can be further lower bounded by $1 - \delta/2$ if M satisfies (4.8).

We next show that for large M , with high probability, the largest q terms of e_j , i.e., $e^{(1)}, \dots, e^{(q)}$, coincide with $\{x_j\}_{j \in [q]}$. Particularly, denoting the index of $e^{(j)}$ as ℓ_j , we will show $[q] = \{\ell_1, \dots, \ell_q\}$. Note that $[q] = \{\ell_1, \dots, \ell_q\}$ if and only if the following probabilistic event occurs:

$$C_q := \left\{ \min_{i \leq q} e_i > \max_{j>q} e_j \right\}.$$

Since for every $i \leq q$ and $j > q$, $e_i - e_j$ is a sum of M i.i.d. random variables Z , where $Z = 1$ with probability $\kappa(x_i)$, $Z = -1$ with probability $\kappa(x_j)$, and $Z = 0$ otherwise. Thus, we can bound the probability of C_q from below with another application of Hoeffding's inequality:

$$\begin{aligned} \mathbb{P}[C_q] &= 1 - \mathbb{P}[C_q^c] \geq 1 - \sum_{i \leq q, j>q} \mathbb{P}[e_i - e_j < 0] \\ &\geq 1 - \sum_{i \leq q, j>q} \mathbb{P}[e_i - e_j - \mathbb{E}[e_i - e_j] < -M\Delta] \\ &\geq 1 - \frac{h^2}{4} \exp \left(-\frac{M\Delta^2}{2} \right) \\ &\geq 1 - \frac{N^2}{4} \exp \left(-\frac{M\Delta^2}{2} \right), \end{aligned}$$

which is lower bounded by $\delta/2$ if M satisfies (4.8). Taking a union bound, for M satisfying (4.8), both the event in (4.10) and C_q occur with probability at least $1 - \delta$.

To finish the proof, it suffices to show that conditional on both events, (i) $\sum_{i \in T} \kappa(x_i) \geq 1 - \eta/2$ and (ii) $|T| \leq \max\{q, d + 1\}$. Let $T_- = T \setminus \{\ell_L\}$. Conditional on the event in (4.10), it follows from the stopping rule in Algorithm 3 that

$$\begin{aligned}
\sum_{j \in T} \kappa(x_j) &\stackrel{(4.10)}{\geq} \sum_{j \in T \cap [q]} \left(\frac{1}{M} e_j - \frac{\eta}{18q} \right) + \sum_{j \in T \cap [N] \setminus [q]} \kappa(x_j) \\
&\geq \sum_{j \in T \cap [q]} \left(\frac{1}{M} e_j - \frac{\eta}{18q} \right) + \sum_{j \in [N] \setminus [q]} \kappa(x_j) - \sum_{j \in [N] \setminus [q]} \kappa(x_j) \\
&\stackrel{(4.10), (4.7)}{\geq} \sum_{j \in T \cap [q]} \left(\frac{1}{M} e_j - \frac{\eta}{18q} \right) + \sum_{j \in [N] \setminus [q]} \frac{1}{M} e_j - \frac{\eta}{18q} - \frac{\eta}{18} \\
&\geq \sum_{j \in T \cap [q]} \left(\frac{1}{M} e_j - \frac{\eta}{18q} \right) + \sum_{j \in T \cap [N] \setminus [q]} \frac{1}{M} e_j - \frac{\eta}{18q} - \frac{\eta}{18} \\
&\geq 1 - \frac{\eta}{3} - \frac{\eta}{18} - \frac{\eta}{18q} - \frac{\eta}{18} > 1 - \frac{\eta}{2},
\end{aligned}$$

which shows that (i) holds true.

To show (ii), it suffices to consider the case where $\min \left\{ \ell : \frac{1}{M} \sum_{j \in [\ell]} e^{(j)} > 1 - \eta/3 \right\} > d + 1$, since otherwise $L = d + 1 \leq \max\{q, d + 1\}$. In this case, the stopping rule in Algorithm 3 tells us

$$\begin{aligned}
\sum_{j \in T_-} \kappa(x_j) &\stackrel{(4.10)}{\leq} \sum_{j \in T_- \cap [q]} \left(\frac{1}{M} e_j + \frac{\eta}{18q} \right) + \sum_{j \in T_- \cap [N] \setminus [q]} \kappa(x_j) \\
&\stackrel{(4.7)}{\leq} \sum_{j \in T_- \cap [q]} \left(\frac{1}{M} e_j + \frac{\eta}{18q} \right) + \frac{\eta}{18} \\
&\leq \sum_{j \in T_-} \frac{1}{M} e_j + \frac{\eta}{18} + \frac{\eta}{18} \stackrel{(4.7)}{<} \sum_{j \in [q]} \kappa(x_j). \tag{4.11}
\end{aligned}$$

Further conditioning on C_q , we have $T_- \subset [q]$ or $[q] \subset T_-$. But the latter cannot happen owing to (4.11).

This implies $|T| = |T_-| + 1 \leq q = \max\{q, d + 1\}$, establishing (ii). \square

5 An approximate AA algorithm

Putting results in Section 3 and 4 together, we have the following approximate algorithm for archetypal analysis (AAA):

Algorithm 4: Approximate Archetypal Analysis (AAA)

Input: $\{x_i\}_{i \in [N]}$: dataset, k : number of archetypes, p : approximation rank, s : Krylov subspace parameter, M : number of projections, η : approximation accuracy

Output: an approximate solution to (1.1)

- 1: generate p random initializations: $\mathbf{S} \in \mathbb{R}^{N \times p}$, $\mathbf{S}_{ij} \stackrel{\text{i.i.d}}{\sim} \mathcal{N}(0, 1)$
- 2: construct the Krylov subspace: $\mathbf{K} = [\mathbf{X}\mathbf{S}, (\mathbf{X}\mathbf{X}^T)\mathbf{X}\mathbf{S}, \dots, (\mathbf{X}\mathbf{X}^T)^{s-1}\mathbf{X}\mathbf{S}] \in \mathbb{R}^{d \times (sp)}$
- 3: compute the QR decomposition for \mathbf{K} : $\mathbf{K} = \mathbf{Q}\mathbf{R}$
- 4: compute the SVD of $\mathbf{X}_{\text{emd}} = \mathbf{X}^T\mathbf{Q}$: $\mathbf{X}_{\text{emd}} = \mathbf{U}_{\text{emd}}\mathbf{\Sigma}_{\text{emd}}\mathbf{V}_{\text{emd}}^T$
- 5: form approximate reduced SVD representation: $\widetilde{\mathbf{X}} = \mathbf{\Sigma}_{\text{emd}}[1:p, 1:p](\mathbf{U}_{\text{emd}}[:, 1:p])^T$
- 6: apply Algorithm 3 to $\widetilde{\mathbf{X}}$ with parameters (M, η) to find a subset of $T \subset [N]$
- 7: solve the reduced archetypal analysis problem:

$$(\widetilde{\mathbf{A}}_\star, \widetilde{\mathbf{B}}_\star) \in \arg \min_{\widetilde{\mathbf{A}} \in \mathbb{R}_{\text{cs}}^{|T| \times k}, \widetilde{\mathbf{B}} \in \mathbb{R}_{\text{cs}}^{k \times N}} \frac{1}{\sqrt{N}} \|\widetilde{\mathbf{X}} - \widetilde{\mathbf{X}}_T \widetilde{\mathbf{A}} \widetilde{\mathbf{B}}\|_F$$

- 8: extend $\widetilde{\mathbf{A}}_\star$ to an $\mathbb{R}^{N \times k}$ matrix by first creating a zero matrix $\mathbf{A}_{\text{null}} \in \mathbb{R}^{N \times k}$, then $\mathbf{A}_{\text{null}}[T, :] \leftarrow \widetilde{\mathbf{A}}_\star$, and finally $\widetilde{\mathbf{A}}_\star \leftarrow \mathbf{A}_{\text{null}}$
 - 9: return $\widetilde{\mathbf{A}}_\star, \widetilde{\mathbf{B}}_\star$
-

Under appropriate assumptions on the input parameters, we have the following guarantee for the solutions computed by Algorithm 4:

Theorem 5.1. *Under the same assumptions in Theorem 4.3 and $p \gtrsim \log(1/\delta)$, if*

$$s \geq C \log \left(\frac{N}{\delta} \right) \quad \eta = \left(\frac{\text{opt}(\mathbf{X})\varepsilon}{\sqrt{2\pi} \max_{i \in [N]} \|x_i\|_2} \right)^{p-1} \quad (5.1)$$

$$M \geq \max \left\{ \frac{324q^2}{\eta^2}, \frac{4}{\Delta^2} \right\} \log \left(\frac{3N}{\sqrt{\delta}} \right), \quad (5.2)$$

where C is the same constant as in Theorem 3.4, $\text{opt}(\mathbf{X})$ is the optimum value of (1.1), q, Δ are the same as defined in Theorem 4.3, then with probability at least $1 - 2\delta$, $|T| \leq \max\{q, p+1\}$, and the approximate archetypes $\mathbf{X}\widetilde{\mathbf{A}}_\star$ as well as the coefficient matrix $\widetilde{\mathbf{B}}_\star$ returned by Algorithm 4 satisfy

$$\frac{1}{\sqrt{N}} \|\mathbf{X} - \mathbf{X}\widetilde{\mathbf{A}}_\star \widetilde{\mathbf{B}}_\star\|_F \leq (1 + \varepsilon) (\text{opt}(\mathbf{X}) + 8\sigma_{p+1}(\mathbf{X})).$$

Remark 5.1. According to Theorem 3.3 and Theorem 4.2, the computational complexity of data dimen-

sionality reduction (step 1 to step 4) and representation cardinality reduction (step 5) is $\mathcal{O}(dNp \log N + \max\{d, N\} \log^2 N p^2)$ and

$$\mathcal{O}(M(pN + N \log N)) = \mathcal{O}(\varepsilon^{-2(p-1)} N \log N (p + \log N) q^2) \leq \mathcal{O}(\varepsilon^{-2(p-1)} N \log^2 N p q^2),$$

respectively. With probability at least $1 - 2\delta$, step 6 solves the reduced problem which has data dimension p and representation cardinality $|T| \leq \max\{p + 1, q\}$. Thus, the overall complexity for Algorithm 4 is small if both p and q are small. This corresponds to the scenario where \mathbf{X} is approximately low-rank and has most of the curvature concentrated on a small subset.

Proof of Theorem 5.1. Let $(\mathbf{A}_\star, \mathbf{B}_\star)$ and $(\widetilde{\mathbf{A}}, \widetilde{\mathbf{B}})$ be solutions to (1.1) and

$$\min_{\mathbf{A} \in \mathbb{R}_{\text{cs}}^{N \times k}, \mathbf{B} \in \mathbb{R}_{\text{cs}}^{k \times N}} \frac{1}{\sqrt{N}} \|\widetilde{\mathbf{X}} - \widetilde{\mathbf{X}} \mathbf{A} \mathbf{B}\|_F, \quad (5.3)$$

respectively. Under the assumptions on η and M , Theorem 4.1 and Theorem 4.3 together imply that with probability at least $1 - \delta$, $|T| \leq \max\{p + 1, q\}$ and

$$\|\widetilde{\mathbf{X}} - \widetilde{\mathbf{X}} \widetilde{\mathbf{A}}_\star \widetilde{\mathbf{B}}_\star\|_F \leq (1 + \varepsilon) \|\widetilde{\mathbf{X}} - \widetilde{\mathbf{X}} \widetilde{\mathbf{A}} \widetilde{\mathbf{B}}\|_F \leq (1 + \varepsilon) \|\widetilde{\mathbf{X}} - \widetilde{\mathbf{X}} \mathbf{A}_\star \mathbf{B}_\star\|_F. \quad (5.4)$$

Let $\widetilde{\mathbf{X}}_p = \widetilde{\mathbf{U}}_p \widetilde{\mathbf{X}}$ and $\widetilde{\mathbf{X}}_p = \mathbf{X} - \widetilde{\mathbf{X}}_p$, where $\widetilde{\mathbf{U}}_p$ is the same as defined in (3.11). For s satisfying (5.1), it follows from Lemma 3.1 that with probability at least $1 - \delta$,

$$\|\widetilde{\mathbf{X}}_{-p}\|_2 = \|\mathbf{X} - \widetilde{\mathbf{X}}_p\|_2 \leq 2\|\mathbf{X} - \mathbf{X}_p\|_2 = 2\sigma_{p+1}(\mathbf{X}), \quad (5.5)$$

where \mathbf{X}_p is the best rank- p approximation for \mathbf{X} . Thus, both (5.4) and (5.5) hold with probability $1 - 2\delta$. Now condition on (5.4) and (5.5). The rest of the proof is completed by a similar computation

as (3.4):

$$\begin{aligned}
\|\mathbf{X} - \mathbf{X}\tilde{\mathbf{A}}_\star\tilde{\mathbf{B}}_\star\|_F &\leq \|\tilde{\mathbf{X}}_p - \tilde{\mathbf{X}}_p\tilde{\mathbf{A}}_\star\tilde{\mathbf{B}}_\star\|_F + \|\tilde{\mathbf{X}}_{-p} - \tilde{\mathbf{X}}_{-p}\tilde{\mathbf{A}}_\star\tilde{\mathbf{B}}_\star\|_F \\
&= \|\tilde{\mathbf{X}} - \tilde{\mathbf{X}}\tilde{\mathbf{A}}_\star\tilde{\mathbf{B}}_\star\|_F + \|\tilde{\mathbf{X}}_{-p} - \tilde{\mathbf{X}}_{-p}\tilde{\mathbf{A}}_\star\tilde{\mathbf{B}}_\star\|_F \\
&\stackrel{(5.4)}{\leq} (1 + \varepsilon) \|\tilde{\mathbf{X}} - \tilde{\mathbf{X}}\mathbf{A}_\star\mathbf{B}_\star\|_F + \|\tilde{\mathbf{X}}_{-p} - \tilde{\mathbf{X}}_{-p}\tilde{\mathbf{A}}_\star\tilde{\mathbf{B}}_\star\|_F \\
&= (1 + \varepsilon) \|\tilde{\mathbf{X}}_p - \tilde{\mathbf{X}}_p\mathbf{A}_\star\mathbf{B}_\star\|_F + \|\tilde{\mathbf{X}}_{-p} - \tilde{\mathbf{X}}_{-p}\tilde{\mathbf{A}}_\star\tilde{\mathbf{B}}_\star\|_F \\
&\leq (1 + \varepsilon) \|\mathbf{X} - \mathbf{X}\mathbf{A}_\star\mathbf{B}_\star\|_F + (1 + \varepsilon) \|\tilde{\mathbf{X}}_{-p} - \tilde{\mathbf{X}}_{-p}\mathbf{A}_\star\mathbf{B}_\star\|_F + \|\tilde{\mathbf{X}}_{-p} - \tilde{\mathbf{X}}_{-p}\tilde{\mathbf{A}}_\star\tilde{\mathbf{B}}_\star\|_F \\
&\stackrel{(3.5)}{\leq} (1 + \varepsilon) \left(\|\mathbf{X} - \mathbf{X}\mathbf{A}_\star\mathbf{B}_\star\|_F + 2\|\tilde{\mathbf{X}}_{-p}\|_F + 2\sqrt{N}\|\tilde{\mathbf{X}}_{-p}\|_2 \right) \\
&\leq (1 + \varepsilon) \left(\|\mathbf{X} - \mathbf{X}\mathbf{A}_\star\mathbf{B}_\star\|_F + 4\sqrt{N}\|\tilde{\mathbf{X}}_{-p}\|_2 \right) \\
&\stackrel{(5.5)}{\leq} (1 + \varepsilon) \left(\|\mathbf{X} - \mathbf{X}\mathbf{A}_\star\mathbf{B}_\star\|_F + 8\sigma_{p+1}(\mathbf{X})\sqrt{N} \right).
\end{aligned}$$

Dividing both sides by \sqrt{N} yields the desired result. \square

6 Numerical experiments

In this section, we apply the proposed algorithm (Algorithm 4) to compute the archetypes for two real datasets, including a time series dataset and an image dataset. When implementing the alternating minimization algorithm for solving AA, we use the k -means centers (computed by the ‘`kmeans`’ function in R) as the initial guess for the archetypes; the subproblems are solved using the existing package ‘`quadprog`’ [42] in R [33]. The algorithm stops if the relative objective decrease falls below $1\text{e-}3$. We will compare the computation time and accuracy of the following algorithms:

- (SVD-AA): Alternating minimization applied to the reduced singular value representation of \mathbf{X} as in (3.1), where truncation keeps 99.9% of the variance of the data. SVD is implemented using the built-in function ‘`svd`’ in R.
- (AAA): Approximate archetypal analysis (Algorithm 4), with $s = \lceil \log N \rceil$.
- (archetypes): A function for archetypal analysis in the package `archetypes` [14, 15] in R, whose implementation is different from Algorithm 1.

To ensure comparability of the results, we do not include other accelerated algorithms such as the active-subset solver [6] and the coresets approximation [26], which have a different focus than our methods. All reported results in this section were obtained on a Macbook Air with a M1 processor and 8GB of RAM.

6.1 S&P 500 cumulative log-returns

The Standard and Poor’s 500 (S&P 500) is a stock market index consisting of 500 large companies listed on stock exchanges in the United States. It is one of the most commonly used equity indices to evaluate the financial market as well as the economy. The companies that are selected for the S&P 500 index are changing with time. In this example, we consider a dataset comprised of 572 companies that were/are chosen for the S&P 500 index from January 2011 to December 2018. In particular, each column in \mathbf{X} corresponds to a 2012-dimensional time series representing the cumulative log-return (which is calculated on a daily basis) (CLR) of a company over eight years. Visualization of the dataset is given in Figure 2. In the rest of the section, we assume that the CLR of each company in the S&P 500 index can be decomposed with respect to a few distinct growth patterns that can be identified via archetypal analysis.

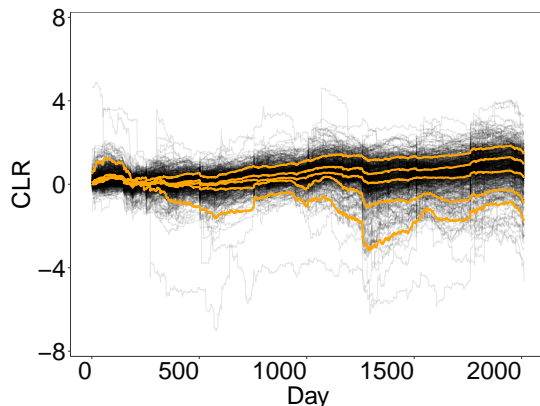


Figure 2: Cumulative log-return (CLR) of 572 S&P 500 stocks from January 2011 to December 2018. Orange curves are the centers of the kmeans applied to \mathbf{X} with $k = 5$.

Let $k = 5$. This choice is quite arbitrary, but we keep it small to enhance interpretability of the analysis. We apply SVD-AA, AAA and archetypes to compute the archetypes for \mathbf{X} . The parameters p , M and η in AAA are set as 50, 10000 and 0.003 (so that $\eta/3 = 0.001$), respectively. Each experiment is repeated 50 times, with the learned archetypes (in the first 12 experiments), the running times (elapsed time computed using the ‘`system.time()`’ function in R) and residuals reported in Figure 3 and Figure 4, respectively.

It can be seen from Figure 4 that SVD-AA, as expected, gives the best computed archetypes in terms of the residual on average (there is an outlier due to the non-convexity of the problem); however, its computation time is significantly longer than the other two methods. The built-in function archetypes has the worst performance, and its computation time is between the other two methods. The AAA, which first

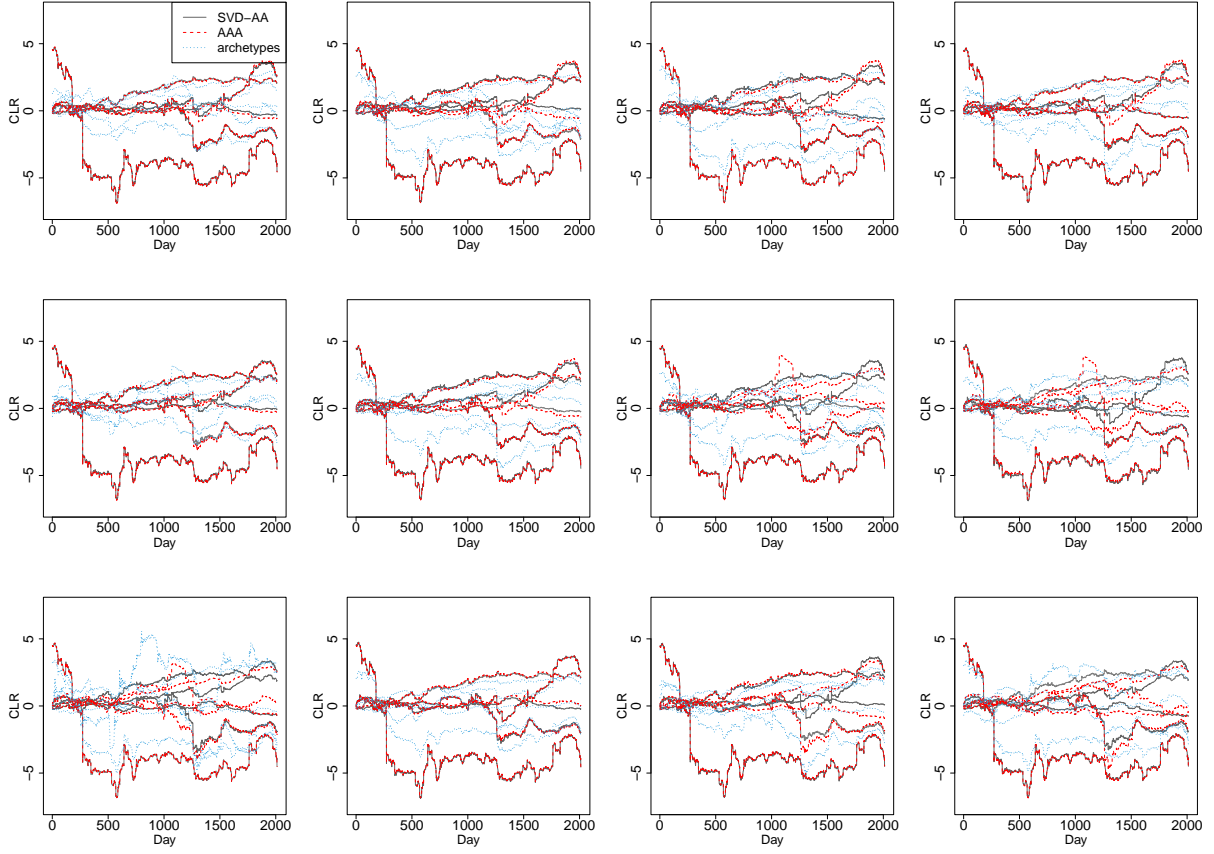


Figure 3: Instances of the computed archetypes by SVD-AA, AAA and archetypes in the first 12 experiments.

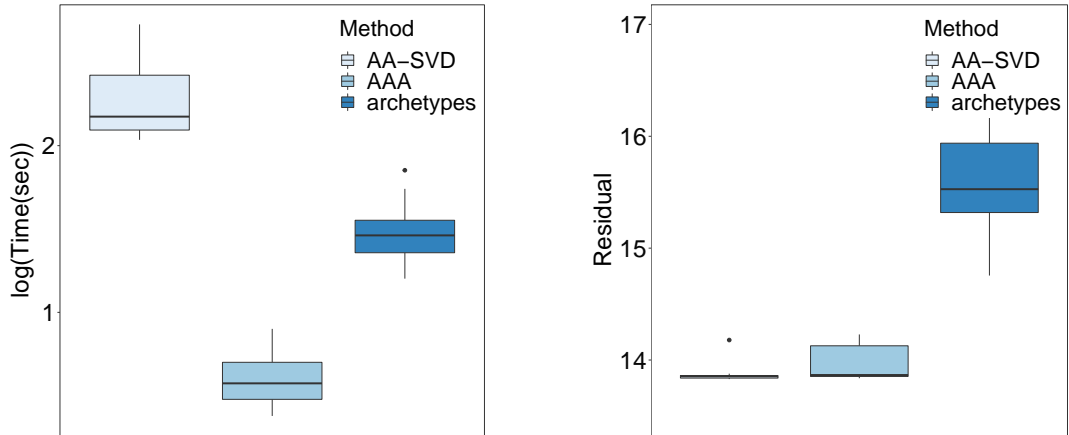


Figure 4: Boxplots of the running times (left) and residuals (right) of SVD-AA, AAA and archetypes in 50 experiments.

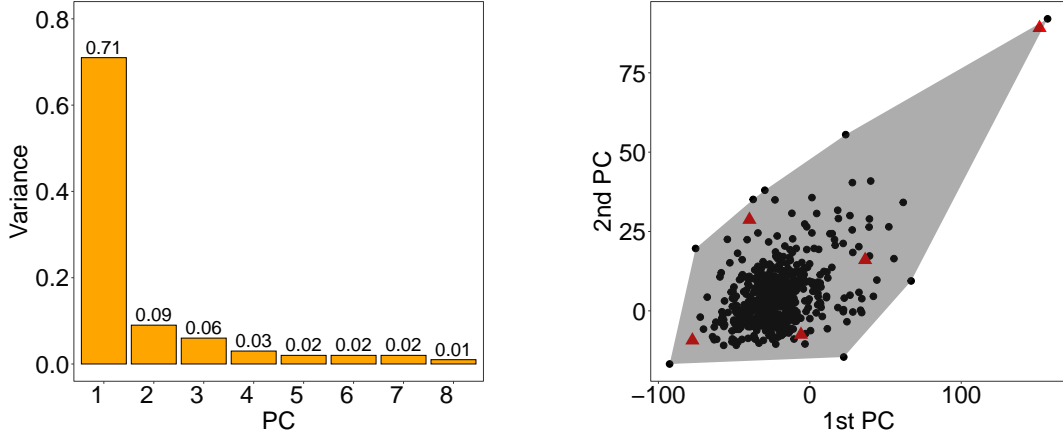


Figure 5: Variances explained by the first 8 principal components of \mathbf{X} (left). Scatterplot of the reduced representation of \mathbf{X} with respect to the first two left singular vectors (which account for 80% of the variation of the dataset) and its convex hull. The red triangles are the reduced representation of the five archetypes (right).

reduces the dimension of the dataset before applying the alternating minimization, achieves competitive results with SVD-AA, but takes much less time (more than 60 times faster than SVD-AA). This may be due to the fact that \mathbf{X} is essentially low-dimensional and admits a parsimonious approximation for its convex hull. A heuristic justification for this argument can be seen from the spectral decay of the sample covariance matrix of \mathbf{X} as well as the scatterplot of the reduced representation of \mathbf{X} with respect to the first two principal components (PCs), as illustrated in Figure 5.

To implement AAA, it necessary to choose the input parameters in advance. The optimal choice for the parameters is problem-dependent and often there is no universal tuning strategy for it. The Krylov subspace parameter s is set as $\lceil \log N \rceil$ deterministically. We investigate the accuracy/running time dependence on p, M and η . In particular, we will use the same parameters as in the previous simulation. Every time when we test the dependence on one parameter, the other two are set fixed. We will test p, M and η at three different values, respectively, i.e., $p = 10, 30, 50$, $M = 10^3, 10^4, 10^5$ and $\eta = 0.3, 0.03, 0.003$. The results are given in Figure 6.

Figure 6 shows that for the S&P 500 dataset, the accuracy of AAA has a strong dependence on η , which measures the missing proportion of curvature in the approximate convex hull construction. The number of random projections M mostly influences the running time while has only a mild impact on the accuracy. The approximation rank p , as long as set reasonably large, is sufficient to give a good approximation result.

In this example, the five true archetypes are visually more illustrative than the centers given by the k -means (with the same k), four of which share a similar growth pattern (Figure 2). Indeed, the

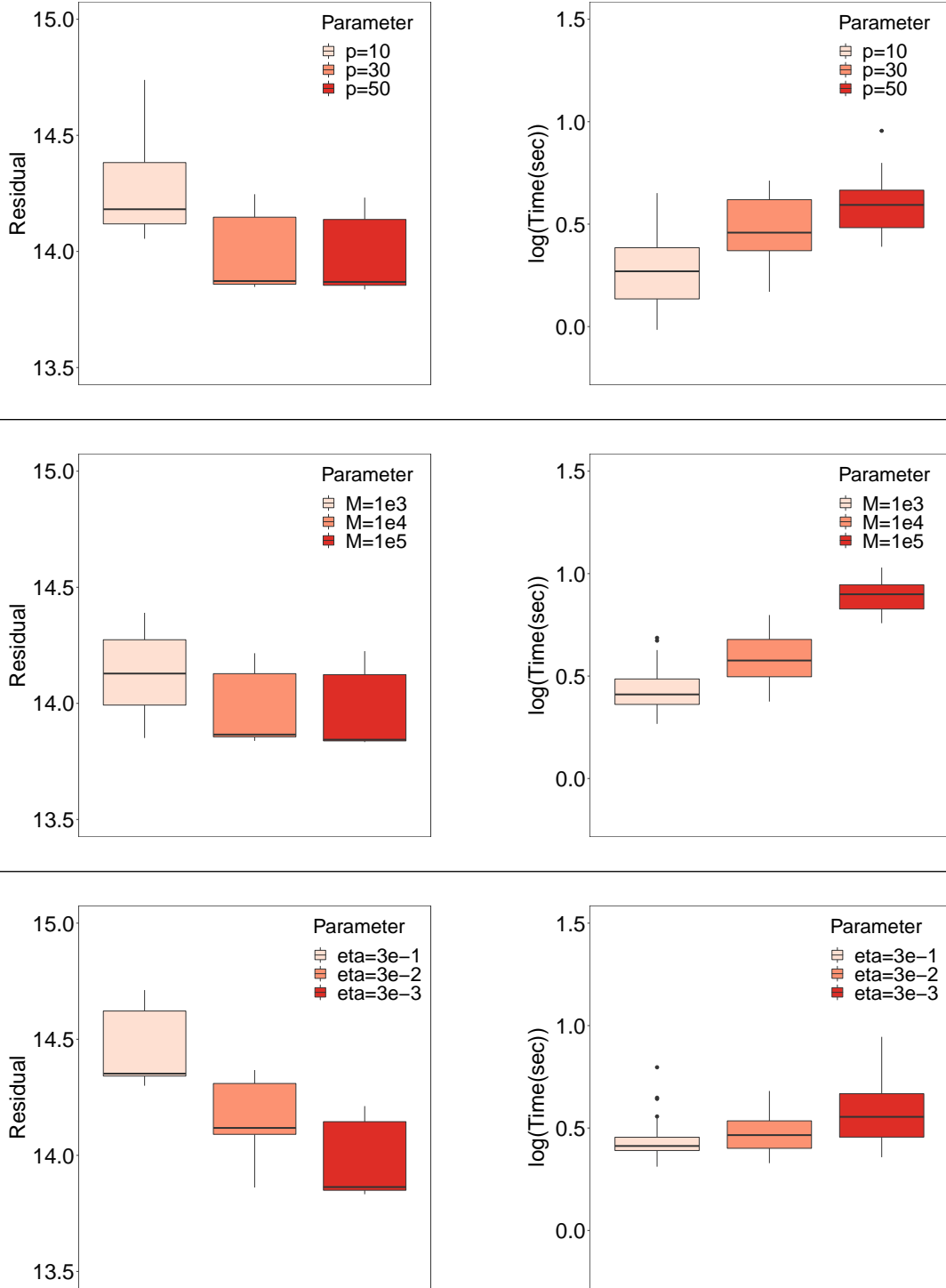


Figure 6: Accuracy/running time dependence of AAA algorithm for the S&P 500 dataset with base parameters $p = 50$, $M = 10^4$ and $\eta = 0.003$.

percentage of variance explained by AA is around 78%; the same number for the k -means and PCA are 40% and 91%, respectively. By computing the coefficients of each column in \mathbf{X} with respect to the archetypes, we find that the five companies having the largest component in each archetype (indexed by their terminal CLR in the decreasing order) are “NVDA”, “REGN” , “FE”, “CLF” and “YRCW”. The five companies are distinct and representative in terms of industries and financial characteristics. Nvidia (NVDA) is an IT company; Regeneron Pharmaceuticals (REGN) is a pharmaceutical company; First Energy (FE) is an electricity company; Cleveland-cliff (CLF) is an ore mining company; Yellow (YRCW) provides transportation services. The five stocks are very different in profitability (whether the business is currently profitable), growth (whether the business has high growth potentials), value (whether the current stock price is relatively low to its revenue), and momentum (whether the stock price maintains a growing trend). Financial analysis shows that both Nvidia (NVDA) and Regeneron Pharmaceuticals (REGN) are very profitable, while Cleveland-cliff (CLF) has great growth potentials. As a utility company, Yellow’s (YRCW) is considered a value stock. First Energy (FE), whose stock return is much higher than its peers in the same industry, is a momentum stock.

6.2 Intel Image

The Intel Image dataset [21] has been used for multi-class classification in machine learning, and consists of 24000 images representing 6 different categories of scene: Buildings, Forest, Glacier, Mountain, Sea and Street. Each image is a 150×150 pixel color image, which corresponds to a 67500-dimensional vector through vectorization and stacking of the pixel matrices ($d = 67500$). We randomly select 3000 samples in the training dataset and apply AAA to extract representative patterns ($N = 3000$). (We could have used the full dataset; however, this would require using a more efficient optimization solver for the subproblems to ensure the computation is done in reasonable time.) We set $k = 10$. The input parameters for AAA are chosen as $p = 10$, $M = 10^5$ and $\eta = 0.003$.

In Figure 7, the 10 archetypes account for about 44% of the variance of the dataset. The instance running time for AAA is 348.784s (85.012s for data dimensionality reduction, 4.715s for representation cardinality reduction and 259.057s for solving the reduced problem using Algorithm 1). In this case, the cardinality of the extreme points used to build up the approximate convex hull is 591. The other two methods, SVD-AA and archetypes, cannot be implemented within reasonable time.

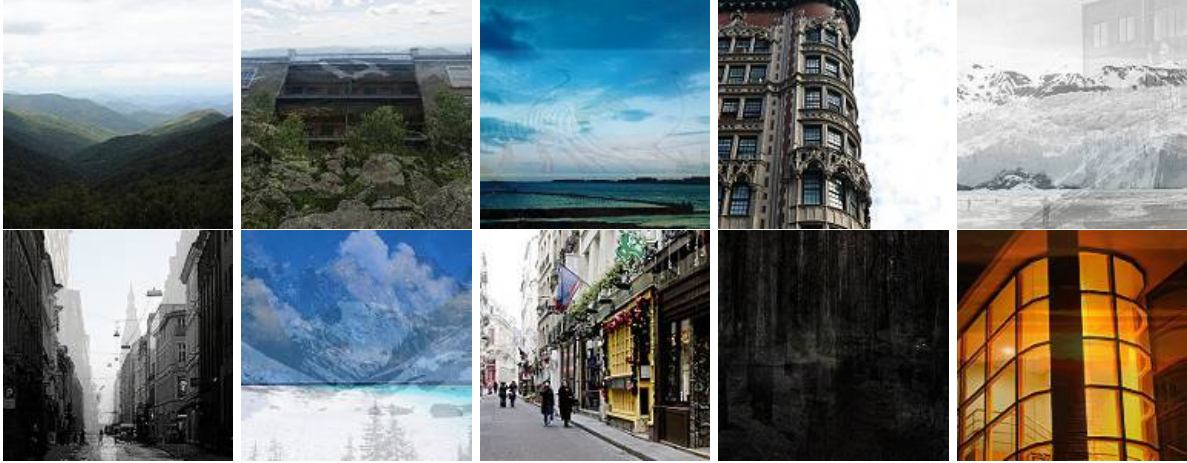


Figure 7: Ten archetypes computed by AAA (with $k = 10$) for the 3000 randomly selected images in the Intel Image dataset.

Acknowledgements

We would like to thank Yu Zhu for providing us with the S&P 500 dataset and helping clarify some related questions. We also thank Akil Narayan for reading through an early draft. Y. Xu would like to thank the organizers of the MSRI Summer Graduate School on Mathematics of Big Data: Sketching and (Multi-) Linear Algebra for motivating discussions.

Funding

R. Han is supported by the Direct Grant for Research from The Chinese University of Hong Kong, Hong Kong under Grant No. 4053474. B. Osting is supported by the National Science Foundation under Grant No. DMS-1752202. D. Wang is supported by the University Development Fund from The Chinese University of Hong Kong, Shenzhen under Grant No. UDF01001803. Y. Xu is supported by the National Science Foundation under Grant No. DMS-1848508.

References

- [1] V. Abrol and P. Sharma. “A geometric approach to archetypal analysis via sparse projections”. In: *International Conference on Machine Learning*. PMLR. 2020, pp. 42–51.
- [2] H. Avron, P. Maymounkov, and S. Toledo. “Blendenpik: Supercharging LAPACK’s least-squares solver”. *SIAM J. Sci. Comput.* 32.3 (2010), pp. 1217–1236.

- [3] C. Battaglini, G. Ballard, and T. G. Kolda. “A practical randomized CP tensor decomposition”. *SIAM J. Matrix Anal. Appl.* 39.2 (2018), pp. 876–901.
- [4] C. Bauckhage, K. Kersting, F. Hoppe, and C. Thureau. “Archetypal analysis as an autoencoder”. In: *Workshop New Challenges in Neural Computation*. Citeseer. 2015, p. 8.
- [5] C. Boutsidis, A. Zouzias, and P. Drineas. “Random Projections for k -means Clustering”. *Advances in Neural Information Processing Systems* 23 (2010), pp. 298–306.
- [6] Y. Chen, J. Mairal, and Z. Harchaoui. “Fast and robust archetypal analysis for representation learning”. In: *Proceedings of the IEEE Conference on Computer Vision and Pattern Recognition*. 2014, pp. 1478–1485.
- [7] K. L. Clarkson and D. P. Woodruff. “Low-rank approximation and regression in input sparsity time”. *J. ACM* 63.6 (2017), pp. 1–45.
- [8] M. B. Cohen, S. Elder, C. Musco, C. Musco, and M. Persu. “Dimensionality reduction for k -means clustering and low rank approximation”. In: *Proceedings of the forty-seventh annual ACM symposium on Theory of computing*. 2015, pp. 163–172.
- [9] A. Cutler and L. Breiman. “Archetypal analysis”. *Technometrics* 36.4 (1994), pp. 338–347.
- [10] A. Damle and Y. Sun. “A geometric approach to archetypal analysis and nonnegative matrix factorization”. *Technometrics* 59.3 (2017), pp. 361–370.
- [11] P. Drineas, M. W. Mahoney, S. Muthukrishnan, and T. Sarlós. “Faster least squares approximation”. *Numer. Math.* 117.2 (2011), pp. 219–249.
- [12] C. Eckart and G. Young. “The approximation of one matrix by another of lower rank”. *Psychometrika* 1.3 (1936), pp. 211–218.
- [13] N. B. Erichson, A. Mendible, S. Wihlbom, and J. N. Kutz. “Randomized nonnegative matrix factorization”. *Pattern Recognition Letters* 104 (2018), pp. 1–7.
- [14] M. J. A. Eugster and F. Leisch. “From Spider-Man to Hero – Archetypal Analysis in R”. *Journal of Statistical Software* 30.8 (2009), pp. 1–23.
- [15] M. J. A. Eugster and F. Leisch. “Weighted and Robust Archetypal Analysis”. *Comput. Statist. Data Anal.* 55.3 (2011), pp. 1215–1225.
- [16] R. Graham and A. M. Oberman. “Approximate Convex Hulls: sketching the convex hull using curvature”. *arXiv preprint arXiv:1703.01350* (2017).
- [17] N. Halko, P.-G. Martinsson, and J. A. Tropp. “Finding structure with randomness: Probabilistic algorithms for constructing approximate matrix decompositions”. *SIAM Rev.* 53.2 (2011), pp. 217–288.
- [18] T. Hastie, R. Tibshirani, and J. Friedman. *The Elements of Statistical Learning*. Springer Series in Statistics. New York, NY, USA: Springer New York Inc., 2001.

- [19] C. A. Hoare. “Quicksort”. *Comput. J.* 5.1 (1962), pp. 10–16.
- [20] W. Hoeffding. “Probability Inequalities for Sums of Bounded Random Variables”. *J. Amer. Statist. Assoc.* 58.301 (1963), pp. 13–30.
- [21] Intel. *Intel image classification challenge*. Public dataset available at <https://www.kaggle.com/puneet6060/intel-image-classification>.
- [22] H. Javadi and A. Montanari. “Nonnegative matrix factorization via archetypal analysis”. *J. Amer. Statist. Assoc.* 115.530 (2020), pp. 896–907.
- [23] M. K. Kozlov, S. P. Tarasov, and L. G. Khachiyan. “Polynomial solvability of convex quadratic programming”. In: *Doklady Akademii Nauk*. Vol. 248. 5. Russian Academy of Sciences. 1979, pp. 1049–1051.
- [24] P. D. Lax. “Functional Analysis. John Wiley&Sons”. *Inc. Publication* (2002).
- [25] S. Mair, A. Boubekki, and U. Brefeld. “Frame-based data factorizations”. In: *International Conference on Machine Learning*. PMLR. 2017, pp. 2305–2313.
- [26] S. Mair and U. Brefeld. “Coresets for Archetypal Analysis”. *Advances in Neural Information Processing Systems* 32 (2019), pp. 7247–7255.
- [27] K. Makarychev, Y. Makarychev, and I. Razenshteyn. “Performance of Johnson-Lindenstrauss transform for k-means and k-medians clustering”. In: *Proceedings of the 51st Annual ACM SIGACT Symposium on Theory of Computing*. 2019, pp. 1027–1038.
- [28] J. Mei, C. Wang, and W. Zeng. “Online dictionary learning for approximate archetypal analysis”. In: *Proceedings of the European Conference on Computer Vision (ECCV)*. 2018, pp. 486–501.
- [29] M. Mørup and L. K. Hansen. “Archetypal analysis for machine learning and data mining”. *Neurocomputing* 80 (2012), pp. 54–63.
- [30] C. Musco and C. Musco. “Randomized block Krylov methods for stronger and faster approximate singular value decomposition”. *Advances in Neural Information Processing Systems* 2015 (2015), pp. 1396–1404.
- [31] B. Ousting, D. Wang, Y. Xu, and D. Zosso. “Consistency of archetypal analysis”. *SIAM J. Math. Data Sci.* 3.1 (2021), pp. 1–30.
- [32] Y. Qian, C. Tan, N. Mamoulis, and D. W. Cheung. “Dsanls: Accelerating distributed nonnegative matrix factorization via sketching”. In: *Proceedings of the Eleventh ACM International Conference on Web Search and Data Mining*. 2018, pp. 450–458.
- [33] R Core Team. *R: A Language and Environment for Statistical Computing*. R Foundation for Statistical Computing. Vienna, Austria, 2020.
- [34] V. Rokhlin, A. Szlam, and M. Tygert. “A randomized algorithm for principal component analysis”. *SIAM J. Matrix Anal. Appl.* 31.3 (2010), pp. 1100–1124.

- [35] M. Rudelson and R. Vershynin. “The Littlewood–Offord problem and invertibility of random matrices”. *Adv. Math.* 218.2 (2008), pp. 600–633.
- [36] H. Rutishauser. “Simultaneous iteration method for symmetric matrices”. *Numer. Math.* 16.3 (1970), pp. 205–223.
- [37] T. Sarlos. “Improved approximation algorithms for large matrices via random projections”. In: *2006 47th Annual IEEE Symposium on Foundations of Computer Science (FOCS’06)*. IEEE. 2006, pp. 143–152.
- [38] O. Shoval, H. Sheftel, G. Shinar, Y. Hart, O. Ramote, A. Mayo, E. Dekel, K. Kavanagh, and U. Alon. “Evolutionary trade-offs, Pareto optimality, and the geometry of phenotype space”. *Science* 336.6085 (2012), pp. 1157–1160.
- [39] C. Thureau, K. Kersting, M. Wahabzada, and C. Bauckhage. “Convex non-negative matrix factorization for massive datasets”. *Knowledge and information systems* 29.2 (2011), pp. 457–478.
- [40] L. N. Trefethen and D. Bau III. *Numerical linear algebra*. Vol. 50. Siam, 1997.
- [41] J. A. Tropp, A. Yurtsever, M. Udell, and V. Cevher. “Practical sketching algorithms for low-rank matrix approximation”. *SIAM J. Matrix Anal. Appl.* 38.4 (2017), pp. 1454–1485.
- [42] B. A. Turlach and A. Weingessel. *quadprog: Functions to solve Quadratic Programming Problems*. R package version 1.5-4. 2011.
- [43] R. Vershynin. *High-dimensional probability: An introduction with applications in data science*. Vol. 47. Cambridge university press, 2018.
- [44] Y. Wang, H. Tung, A. Smola, and A. Anandkumar. “Fast and Guaranteed Tensor Decomposition via Sketching”. In: *NIPS*. 2015.
- [45] D. P. Woodruff. “Sketching as a Tool for Numerical Linear Algebra”. *Foundations and Trends® in Theoretical Computer Science* 10.1–2 (2014), pp. 1–157.